Hydrogen as a Modifier of the Structure and Electronic Properties of Platinum in Acidic Zeolite LTL: A Combined Infrared and X-ray Absorption Spectroscopy Study

Marius Vaarkamp,*[†,§] Barbara L. Mojet,[†] Menno J. Kappers,[†] Jeff T. Miller,[‡] and Diek C. Koningsberger[†]

Debye Institute, Department of Inorganic Chemistry, Utrecht University, P.O. Box 80083, 3508 TB Utrecht, The Netherlands, and Amoco Oil Company, Amoco Research Center, 150 W. Warrenville Rd., Naperville, Illinois 60566-7011

Received: June 2, 1995; In Final Form: August 22, 1995[⊗]

The structure and electronic properties of platinum in Pt/H−LTL after reduction at 300 °C and heating in helium to 500 or 690 °C were determined using X-ray absorption and infrared spectroscopy. After reduction at 300 °C, the platinum particles were metallic, consisted of 4 or 5 atoms, and were located at 2.64 Å from the oxygen atoms in the zeolite framework. The particles remained metallic but increased in size to ≈13 atoms during hydrogen desorption by heating in a helium flow up to 690 °C. Simultaneously, the distance between metal particle and oxygen atoms of the zeolite framework was shortened to 2.05 Å. After reduction at 300 °C and in the presence of chemisorbed hydrogen, the platinum atoms in the PT/H−LTL catalyst had more holes in the d-band than bulk platinum. Hydrogen desorption decreased the number of holes of the platinum atoms in the Pt/H−LTL catalyst to levels lower than bulk metal values. The linear CO band shifted from 2071 to 2084 cm^{-1} upon hydrogen desorption, due to the increased particle size and/or the change in the structure of the metal−support interface. The apparent contradiction between the shift to higher wavenumbers of the linear CO band and the decreased number of holes in the d-band was attributed to the interaction of CO with filled d-orbitals and the effect of chemisorbed hydrogen on the distribution of the local density of states.

Introduction

The influence of the reduction temperature on the average particle size in supported metal catalysts has been firmly established, i.e., higher reduction temperatures result in larger particles. However, the accompanying changes in catalytic properties are difficult to rationalize on the basis of geometric arguments only. For example, reduction at high temperature decreases the specific hydrogenolysis activity of platinum on acidic and neutral supports.[1,2] The decreased activity has been attributed to the poisoning of catalytically active sites by strongly chemisorbed hydrogen[1] or the desorption of hydrogen from the metal−support interface which modifies the metal−support interaction.[2]

Temperature-programmed desorption of hydrogen from supported noble metal catalysts reduced at low temperature (≤300 °C) shows that at least four different types of hydrogen are present. Hydrogen desorptions below 300 °C are reversible and due to chemisorbed hydrogen. Higher temperature peaks of H/Pt stoichiometries up to 4 have been reported. Desorptions with H/Pt stoichiometries below 1 have been assigned to the desorption of strongly adsorbed hydrogen,[3] subsurface hydrogen,[4] and hydrogen evolving from the metal−support interface.[2] Desorptions with higher H/Pt stoichiometries have been attributed to spillover hydrogen[2,5] and hydrogen produced by the oxidation of metallic particles by support protons.[6,7]

The conflicting assignments of the high-temperature hydrogen desorptions with H/Pt stoichiometries above 1 described above call for a more in-depth characterization of the structural and electronic properties of the catalyst before and after desorption. EXAFS, IR, and white line intensity measurements presented in this paper show that platinum particles in acidic zeolite LTL are metallic before and after hydrogen desorption at high temperature. Simultaneously, a shortening of the distance between metal particle and zeolite framework, a shift to higher wavenumbers of linearly adsorbed CO, and a decrease in the number of holes in the platinum d-band were observed.

Experimental Section

Preparation. The K−LTL zeolite (UOP) was converted into the NH_4^+ form by aqueous ion exchange with 10-fold excess 1.5 M NH_4NO_3 at 80 °C for 2 h. Subsequently, the zeolite was filtered, washed, and calcined at 540 °C for 3 h. The resulting exchanged and calcined zeolite contained 7.3 wt % K and 10.9 wt % Al, corresponding to a K:Al ratio of 0.46. After calcination the zeolite was impregnated by contacting with a tetraamineplatinum(II) nitrate (Johnson Matthey) solution for 3 h at room temperature. The impregnated catalyst was dried overnight at 120 °C and contained 1.2 wt % Pt.

X-ray Absorption Spectroscopy. The lid and sample holder of an in-situ gas treatment cell described by Kampers et al.[8] were modified; a schematic drawing of the (unmodified) body, lid, and sample holder is shown in Figure 1. Previously, heating and cooling of the sample holder were carried out by attaching either a cartridge heater or a Dewar filled with liquid nitrogen to the lid. Although this system is convenient, the approximately 5 cm distance between heating or cooling device and sample holder limits the temperature to which the sample can be heated or cooled, i.e., maximum temperature ≈500 °C and cooling with liquid nitrogen resulted in sample temperatures of ≈−130 °C. In the modified lid and sample holder the direct contact between both heating wire and liquid nitrogen and the sample holder (detail of Figure 1) allows heating of the sample to 690 °C; cooling with liquid nitrogen results in temperatures

[†] Utrecht University.
[‡] Amoco Oil Company.
[§] Present address: Mitsubishi Chemical Corporation, Yokohama Research Center, 1000 Kamoshida-cho, Aoba-ku, Yokohama 227, Japan.
[⊗] Abstract published in *Advance ACS Abstracts,* October 1, 1995.

0022-3654/95/2099-16067$09.00/0

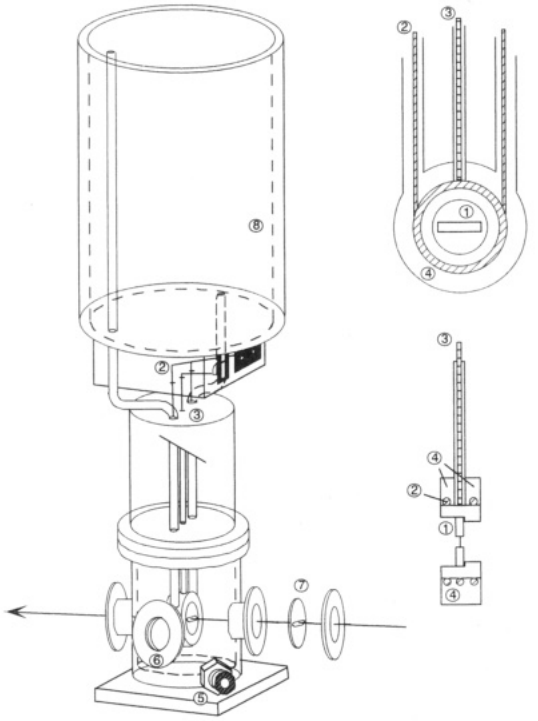

Figure 1. Schematic drawing of the gas treatment cell based on the design of Kampers et al.[8] used for the in-situ XAS and IR spectroscopy measurements: 1, sample holder; 2, coaxial heating wire; 3, thermocouple; 4, space for cooling liquid; 5, water connector; 6, vacuum bellow for connection with gas dose or vacuum system; 7, Be window; 8, Dewar with cooling liquid.

of ≈−190 °C in the sample holder. An additional advantage is a reduction of the mass to cool or heat, which results in faster temperature control. Temperature control of an insulating sample is instantaneous in a gas atmosphere, while in vacuum more than 20 min is needed to reach a steady state temperature due to the absence of the heat transferring gas. During heating the sample is at a higher temperature than the control thermocouple. This offset increases from 0 °C at ambient temperatures to 40 °C at 650 °C. At temperatures below ambient, the control thermocouple and sample temperature are equal. Throughout this paper actual sample temperatures will be reported.

Prior to the XAS experiments, the catalyst was dried in flowing helium at 120 °C for 30 min. After cooling to room temperature (RT), the catalyst was reduced in flowing hydrogen at 300 °C for 1 h (heating rates 3 °C/min). Subsequently, XAS data were collected. Next, a hydrogen TPD was mimicked by switching to a flow of helium and heating the sample at 10 deg/min to 500 °C. After data collection a hydrogen TPD up to 690 °C was mimicked, and XAS data were collected again. All spectra were measured while the sample was cooled with liquid nitrogen; i.e., the sample temperature was −196 °C.

The procedures used to collect XAS spectra and analyze the EXAFS data have been described in detail previously.[9] Using the data of a platinum foil placed between the second and third ion chamber, each spectrum was separately calibrated at the L_{III} and L_{II} edge. To quantify the differences in white line intensity between the catalyst and platinum foil, the method described by Mansour et al.[10] was used. The normalized XAS spectra of the Pt L_{II} and L_{III} edge of platinum foil and the catalyst were aligned at their inflection points. After subtraction of the platinum foil data from the data of the catalyst, the resulting curves were numerically integrated between −2 and +17 eV for both the L_{III} (ΔA_3) and the L_{II} (ΔA_2) edge. Using

$$f_d = \frac{\Delta A_3 \sigma_3 + 1.11 \Delta A_2 \sigma_2}{A_{3r} \sigma_3 + 1.11 A_{2r} \sigma_2} \quad (1)$$

the fractional change in the total number of unfilled states in the d-band of the sample compared to the platinum foil (f_d) was calculated. The areas ΔA_3 and ΔA_2 are multiplied by the corresponding X-ray absorption cross section of platinum at the Pt L_{III} (σ_3, 117.1) and the Pt L_{II} edge (σ_2, 54.2).[11] Values of 7.37 and 0.49 were used for A_{3r} and A_{2r}, respectively.[10] When the number of unfilled d-states in the reference material (h_{Tr}) is known, the number of unfilled d-states in the sample (h_{Ts}) can be calculated from

$$h_{Ts} = (1 + f_d) h_{Tr} \quad (2)$$

For platinum, h_{Tr} was calculated to be 0.3 by Brown et al.[12]

Infrared Spectroscopy. Infrared spectroscopy was performed in the same in-situ gas treatment cell as used for XAS, but equipped with CaF_2 windows to obtain infrared transparency. The cell was connected to an all-metal gas handling system allowing measurements under low pressure ($<10^{-5}$ mbar) as well as under flow conditions. The gases were of high purity; H_2, O_2 (99.995%), He (99.999%), and CO (99.997%, in Al cylinder) were supplied by Hoekloos. Hydrogen and helium were passed through reduced BTS catalysts and dried molecular sieves at 77 K. Oxygen and carbon monoxide were passed through a molecular sieve only.

All infrared spectra were recorded on a Perkin-Elmer 1720-X Fourier transform IR spectrometer equipped with a DTGS detector by coadding 128 scans at a spectral resolution of 2 cm^{-1}. Second derivatives were calculated with a nine-point Savitzky−Golay derivative function.

About 20 mg of catalyst powder was pressed at 2 t into a thin self-supporting wafer with 13 mm diameter and placed in the infrared cell. The fresh catalyst was dried under vacuum at 120 °C for 30 min, ramping the temperature at 3 °C/min. A flow of hydrogen was admitted at ambient temperature, and the sample was reduced at 300 °C for 30 min ramping at 5 °C/min. After cooling to RT under a static atmosphere of hydrogen, the catalyst was exposed to a helium flow at RT and heated to the desired final TPD temperature at a rate of 10 °C/min. Subsequently, the catalyst was cooled in static helium and evacuated for 5 min at room temperature. After recording the infrared spectrum of the catalyst background, 100 mbar of CO was added to the cell and equilibrated for 10 min before the CO gas phase was pumped off (pressure $<10^{-3}$ mbar), and the product spectrum was collected. The background spectrum was digitally subtracted from the product spectrum to obtain the CO absorbance spectrum.

Sample Coding. Data obtained on samples after reduction are indicated by R- followed by the reduction temperature. For example after reduction at 300 °C the code is R-300. Data obtained after mimicking a TPD are indicated by TPD- followed by the final temperature. For example after a helium flush at RT the code is TPD-RT; after heating in helium to 690 °C the code is TPD-690.

Results

EXAFS. The k^1 weighted averaged EXAFS spectrum of R-300 measured in an H_2 atmosphere is shown in Figure 2. EXAFS wiggles are present up to 18 $Å^{-1}$, implying that the quality of the data is very good. The normalized k^1 weighted, Pt−Pt phase- and amplitude-corrected Fourier transform of both a 4 μm platinum foil and R-300 have their main peak at 2.7−2.8 Å (Figure 3), indicating that the platinum in the catalyst is

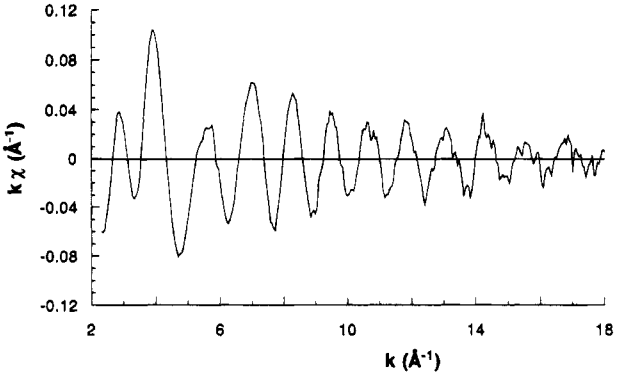

Figure 2. Average k^1 weighted EXAFS of the Pt/H−LTL catalyst dried at 120 °C and reduced at 300 °C (R-300).

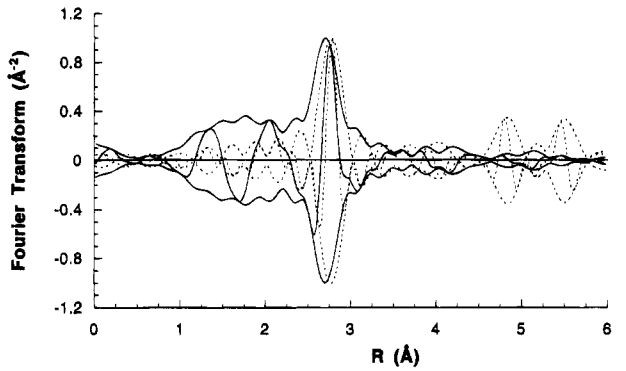

Figure 3. Normalized Fourier transform [k^1, Δk: 3.1−15.2 Å^{-1}; Pt−Pt phase- and amplitude-corrected] of the EXAFS of R-300 (solid line) and the EXAFS of a 4 μm platinum foil (dotted line).

metallic. The shorter distance of the maximum in the Fourier transformed EXAFS of the catalyst indicates a small, but significant, contraction of the Pt−Pt bond distance compared with the bulk Pt−Pt distance. At the low R side of the main peak (1.0−2.5 Å) the difference in the imaginary part of R-300 and the platinum foil provides evidence that, besides platinum, an additional scatterer contributes to the EXAFS of R-300. At higher distances the Fourier transform of the EXAFS of the foil exhibit peaks that are due to higher coordination shells. The absence of these peaks in the Fourier transform of the EXAFS of R-300 indicates that the platinum particles in the catalyst are small.

The three data sets of R-300 were separately background subtracted, normalized, and Fourier filtered (k^2, Δk: 2.7−13.0 Å^{-1}; ΔR: 1.1−3.1 Å). The three Fourier filtered spectra were averaged, resulting in an average Fourier filtered EXAFS spectrum in which the random error in each data point is known. Coordination parameters of the model EXAFS spectrum were optimized in k-space using nonlinear least-squares optimization with analytical partial derivatives.[13] A model EXAFS spectrum with a platinum and an oxygen contribution describes the data well in both k- and R-space (Figure 4). The coordination parameters of these contributions are listed in Table 1 together with the error, calculated from the random error in the data points and the correlation between the parameters.[14]

Assuming a three-dimensional particle geometry, the average platinum particle in R-300 consists of 4 or 5 atoms as inferred from the Pt−Pt coordination number of 3.7. The Pt−Pt distance of 2.74 Å is significantly shorter than the Pt−Pt distance in bulk platinum (2.77 Å); it is however not as short as reported for platinum clusters without chemisorbed hydrogen (2.66 Å).[14−16] In Figure 3 the difference in distance between the maxima in the peaks of R-300 and platinum foil is ≈0.05 Å, which is significantly larger than the decrease in the Pt−Pt

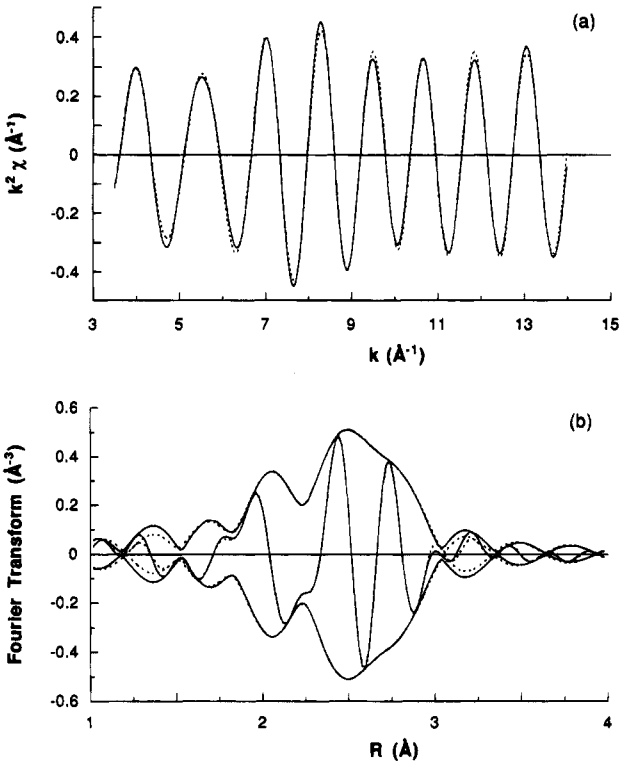

Figure 4. (a) Mean Fourier filtered EXAFS of R-300 (solid line) and the model spectrum (dotted line) calculated with the coordination parameters listed in Table 1. (b) Fourier transform [k^2, Δk: 3.5−13.0 Å^{-1}] of the spectra shown in (a).

TABLE 1: Structural Parameters from EXAFS for Pt/H−LTL after Reduction at 300 °C

backscatterer	N	R (Å)	$\Delta\sigma^2$ (Å^2 × 10^{-3})	ΔE_0 (eV)
Pt	3.7 ± 0.2	2.74 ± 0.01	2.7 ± 0.1	4.0 ± 0.1
O	1.2 ± 0.1	2.64 ± 0.01	2.5 ± 0.2	6.6 ± 0.2

distance found in the refinement. The additional shift in Figure 3 is due to the interference of the Pt−O and Pt−Pt contributions. The oxygen contribution at 2.64 Å is due to the oxygen atoms in the zeolite framework and is in the range of 2.5−2.7 Å generally found for supported noble metal catalysts reduced at temperatures up to 300 °C and covered with hydrogen during the measurement.[17] The high distance compared to the Pt−O distance in oxidic compounds has been attributed to the presence of hydrogen in the platinum−zeolite interface.[9]

The k^1 weighted EXAFS spectra of TPD-500 and TPD-690 are shown in Figure 5a. The noise in these spectra is higher than the noise in the spectrum of R-300 (Figure 2) due to the lower number of scans available, i.e., two for TPD-500 and one for TPD-690. Apart from the different noise level, only small differences in the magnitude of the EXAFS wiggles are present. In the k^1 weighted Fourier transforms (Figure 5b) the main peak is located around 2.6 Å, indicating that the platinum is metallic after desorption of hydrogen at 500 or 690 °C. The amplitude of TPD-690 is higher than the amplitude of TPD-500 in the first and higher shell region, indicating a larger particle size for TPD-690.

A complete analysis of the EXAFS of the Pt/H−LTL catalyst after reduction at 500 °C (R-500) has been reported previously.[9] A comparison of the k^1 weighted, Pt−Pt phase- and amplitude-corrected Fourier transforms of the EXAFS of TPD-500 and R-500 (Figure 6) reveals that the magnitude of the Fourier transform of the EXAFS of TPD-500 is diminished by approximately 50%, indicating either a decrease in number of neighbors or an increase in the disorder. Furthermore, the main

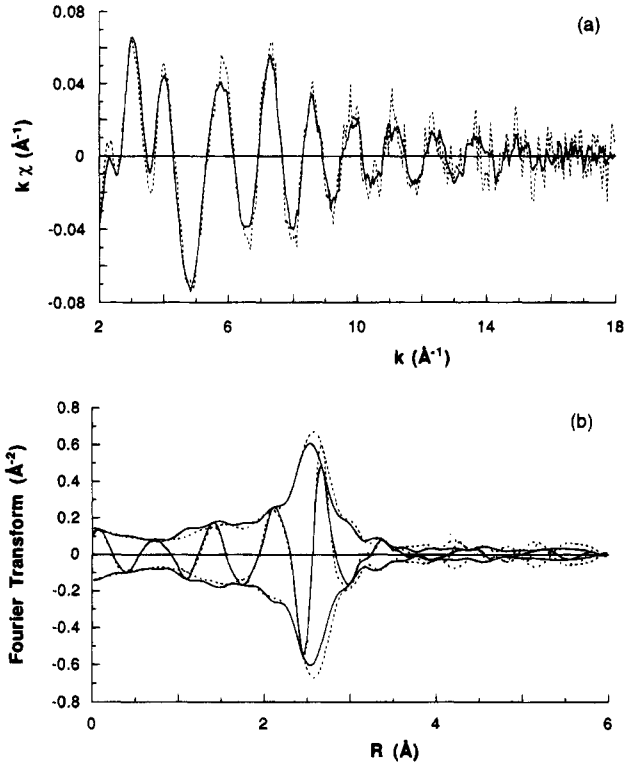

Figure 5. (a) k^1 weighted EXAFS of TPD-500 (solid line) and TPD-690 (dashed line). (b) Fourier transform [k^1, Δk: 3.1−14.2 Å^{-1}, Pt−Pt phase- and amplitude-corrected] of the spectra shown in (a).

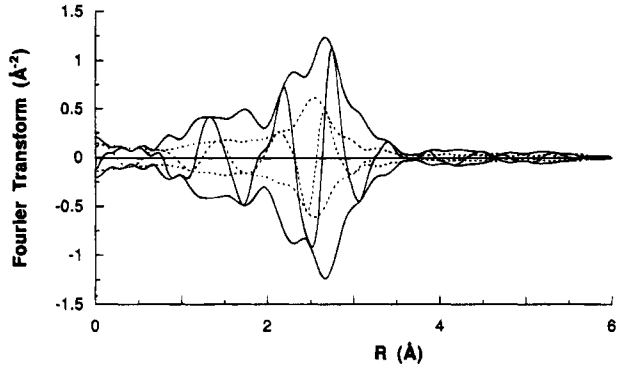

Figure 6. Fourier transform [k^1, Δk: 3.1−14.2 Å^{-1}, Pt−Pt phase- and amplitude-corrected] of TPD-500 (dotted line) and R-500 (solid line).[9]

TABLE 2: Structural Parameters from EXAFS for Pt/H−LTL after Reduction at 300 °C and Subsequent Heating to 500 or 690 °C

scatterer	T_{TPD} (°C)	N	R (Å)	$\Delta\sigma^2$ (Å^2 × 10^{-3})	ΔE_0 (eV)
Pt	500	4.6 ± 0.1	2.60 ± 0.01	6.5 ± 0.1	9.9 ± 0.1
	690	5.6 ± 0.1	2.61 ± 0.01	6.8 ± 0.4	7.6 ± 0.6
O	500	0.2 ± 0.1	2.08 ± 0.01	−0.2 ± 0.2	8.3 ± 0.2
	690	0.2 ± 0.1	2.03 ± 0.01	−3 ± 4	15 ± 5

peak has shifted to lower R, indicating a contraction of the Pt−Pt distance.

The EXAFS spectra of TPD-500 and TPD-690 are described accurately with the parameters listed in Table 2. The Pt−Pt distance is shortened to 2.60 and 2.61 Å, respectively; these values are lower than those reported for naked platinum clusters and the shortest metal−metal distance for platinum particles ever reported. The Pt−Pt coordination number increases with the final TPD temperature and is higher than after reduction at 300 or 500 °C.[9] Note that the disorder values ($\Delta\sigma^2$) also increase. Combination of the decrease in the amplitude

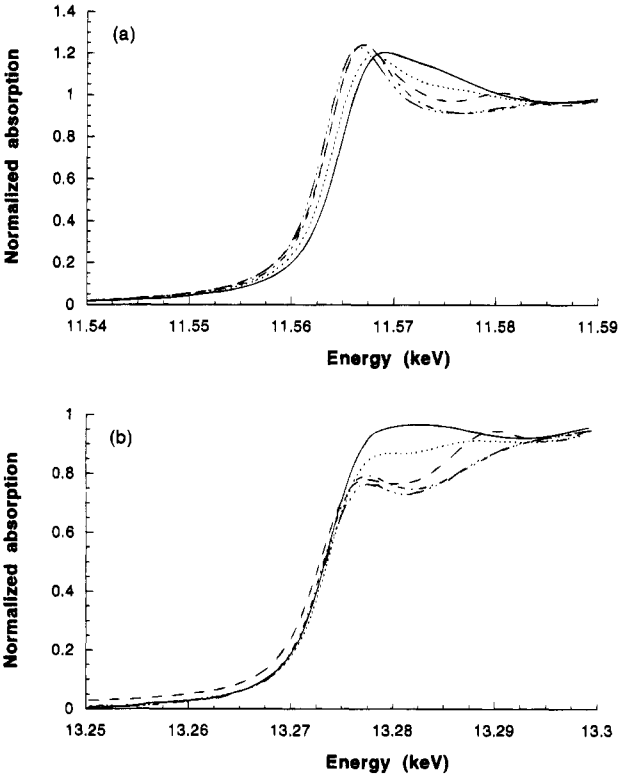

Figure 7. Normalized X-ray absorption of R-300 (solid line), R-500 (dotted line), TPD-500 (dot dash line), TPD-690 (dot dot dot dash line), and platinum foil (dashed line): (a) Pt L_{III} edge, (b) Pt L_{II} edge. In (a) the lines of TPD-500 and TPD-690 nearly coincide.

observed in Figure 6 and the coordination parameters leads to the conclusion that the decrease in amplitude of the EXAFS brought about by the higher disorder is larger than the increase in amplitude due to the higher coordination number. The Pt−O contribution at 2.64 Å that was present in the spectrum of R-300 has vanished. A small contribution at 2.03−2.08 Å is the only indication of interaction between the platinum particles and the supporting zeolite. Although the coordination numbers are low, the significance of the contribution is 92% and 72% for TPD-500 and TPD-690, respectively. Oxygen contributions with distances around 2.05 Å have been reported for reduced Pt/Al_2O_3[18] and Pt/SiO_2[19] catalysts that were flushed with He at high temperature prior to measurement.

X-ray Absorption Edges. The Pt L_{III} and the Pt L_{II} X-ray absorption edges of the Pt/H−LTL catalyst after the various treatments are shown in Figure 7. Spectra of platinum foil and Pt/H−LTL reduced at 500 °C are added for comparison. Clearly, large changes in both intensity and shape of the edges as well as shifts in the position of the edges are present.

The Pt L_{III} and the Pt L_{II} edges of the platinum clusters without chemisorbed hydrogen are sharper than the edges of the clusters with chemisorbed hydrogen and resemble the edge shape of bulk platinum, indicating that chemisorbed hydrogen affects the energy distribution of the empty states in a platinum cluster. Consistent intensities of the Pt L_{III} X-ray absorption edge higher than platinum foil have been reported for platinum clusters supported by zeolite Y[20] and mordenite[21] and measured in the presence of hydrogen. The Pt L_{III} edge position is equal within experimental error for the foil and the catalysts without chemisorbed hydrogen, i.e., TPD-500 and TPD-690. The position of the Pt L_{III} edge of the catalysts with chemisorbed hydrogen, i.e., R-300 and R-500, is located at higher energy than the edge of bulk platinum. For R-300 the shift is 1.0 eV, and for R-500 the shift is 0.5 eV. In contrast, the position of

TABLE 3: Intensity of Pt L_{III} and Pt L_{II} X-ray Absorption Edges of the Pt/H−LTL Catalyst

treatment	ΔA_3	ΔA_2	f_d
H_2, 300 °C	0.6738	1.7169	0.204
He, 500 °C	−0.6357	−0.3957	−0.110
He, 690 °C	−0.7912	−0.6334	−0.146

the Pt L_{II} edge position is not affected by the presence or absence of chemisorbed hydrogen and is equal to the edge position of bulk platinum. Apparently, the interaction of chemisorbed hydrogen with the $5d_{5/2}$ state differs from the interaction with the $5d_{3/2}$ state of platinum. Shifts in edge position due to chemisorbed hydrogen were shown to be reversible,[14,16] indicating that the changes in edge position are related to the interaction of chemisorbed hydrogen with the d-band of the platinum clusters.

Calculation of the number of holes in the d-band of the platinum clusters was performed by alignment of the edge of the sample and platinum foil followed by numerical integration of the difference. The results (Table 3) reveal that the average platinum atom in a cluster with chemisorbed hydrogen has more holes in the d-band than bulk platinum atoms. Atoms in naked clusters have fewer holes in the d-band than bulk platinum atoms. Conversion of the f_d values of R-300 and TPD-690 to the actual number of holes reveals that the difference in holes in the d-band between these samples amount to 0.10 electron per atom. An electron density on metal atoms higher than the electron density in the bulk metal has been reported before for a Pt/γ-Al_2O_3 catalyst with very small platinum particles reduced and evacuated at 300 °C.[14,16]

Infrared Spectroscopy. The IR spectra of carbon monoxide adsorbed on TPD-RT, TPD-150, TPD-300, TPD-500, and TPD-690 show an intense absorption band at 2080−2070 cm^{-1} with a weak shoulder around 2120 cm^{-1} and weak multiple absorptions in the region 1925−1750 cm^{-1} (Figure 8). The intense band is attributed to CO species linearly bonded to Pt atoms, whereas the weaker low-frequency bands are due to bridging CO molecules.[22]

Temperature-programmed hydrogen desorption from the reduced catalyst shifts the CO absorption bands. The maximum of the linear-CO peak for TPD-RT at 2071 cm^{-1} shifts to 2074, 2078, 2081, and 2081 cm^{-1} for TPD-150, TPD-300, TPD-500, and TPD-690, respectively. Simultaneously, the bridge-CO bands at 1845 and 1810 cm^{-1} for TPD-RT shift to respectively 1855 and 1800 cm^{-1} for TPD-500, while a new band appears at 1915 cm^{-1}. The integrated band intensity of linear-CO declines gradually with increasing TPD temperature up to an intensity loss of 10% for TPD-690 with respect to TPD-RT.

The region 2200−2000 cm^{-1} has been further analyzed by calculating the corresponding second derivatives (Figure 9). Each negative peak in the second derivatives corresponds to a specific CO species. Note that the linear-CO bands in Figure 8 extend all the way to ≈1980 cm^{-1}, indicating that more species are present than there are distinct negative peaks in the second derivative.

In the region between 2100 and 2000 cm^{-1}, typical for CO species bound to Pt metal clusters, a broad negative peak, containing some structure, is present indicating the heterogeneity of the surface and the different environment of the adsorption sites. The peak at 2087 cm^{-1} grows steadily with final TPD temperature up to 500 °C, but loses intensity by further increasing the final TPD temperature to 690 °C. After TPD up to 690 °C, the shape of the second-derivative peak has changed into a single broad peak at 2081 cm^{-1}.

The second derivatives also show that the high-frequency shoulder at 2120 cm^{-1} in the original linear-CO bands consist

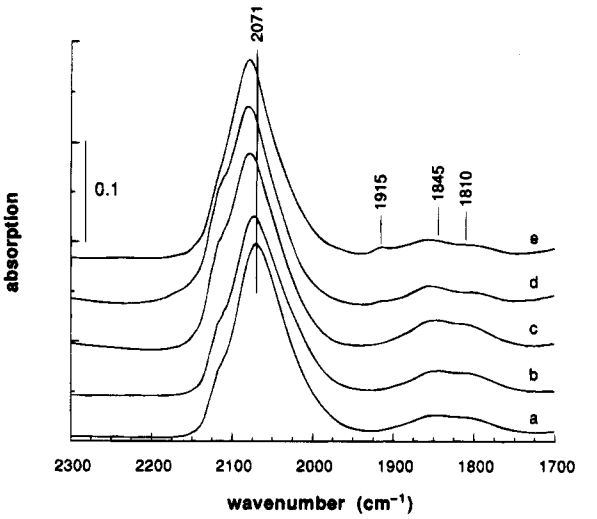

Figure 8. Infrared spectra of CO chemisorbed on (a) TPD-RT, (b) TPD-150, (c) TPD-300, (d) TPD-500, and (e) TPD-690.

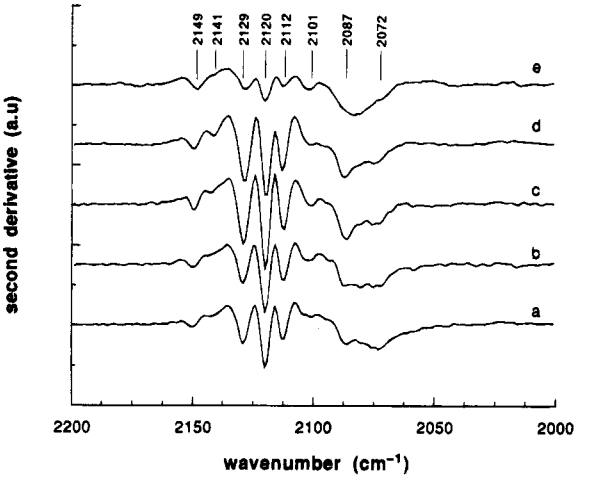

Figure 9. Second derivatives of the spectra in Figure 8.

of at least six distinct peaks at 2149, 2141, 2129, 2120, 2112, and 2101 cm^{-1}. Infrared absorption bands in this region have been attributed to CO adsorbed on oxidized and/or electron−deficient metal sites and/or CO on metal sites that are adjacent to oxygen atoms.[23] No peaks due to adsorbed CO could be distinguished above 2150 cm^{-1}. The intensity of the high-frequency peaks increases with final TPD temperatures up to 300 °C but decreases steadily upon treatment at higher temperatures. Carbon monoxide is weakly bound in these complexes as the bands are strongly suppressed upon prolonged evacuation at RT.

Three checks were made to assess the validity of the IR results. First, the influence of water on the zeolite hydroxyl groups and protons and the position of the linear CO bands were determined. Second, the IR spectrum of CO adsorbed on a reduced sample that was exposed to oxygen was measured. Third, the reversibility of the hydrogen desorption was examined.

The total absorption in the hydroxyl region decreases with increasing final TPD temperature (Figure 10), due to desorption of water. Simultaneously, the peak due to terminal silanol groups at 3746 cm^{-1} sharpens and increases in intensity. Absorption peaks due to the presence of protons and/or silanol groups inside the zeolite are located at 3630 and 3675 cm^{-1}. The peak at 3630 cm^{-1} is better resolved after TPD up to 500 °C but loses intensity during TPD to 690 °C. The peaks at

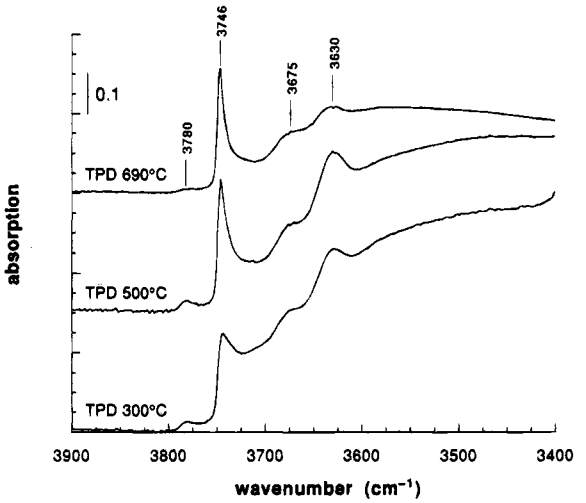

Figure 10. Hydroxyl region of TPD-300, TPD-500, and TPD-690.

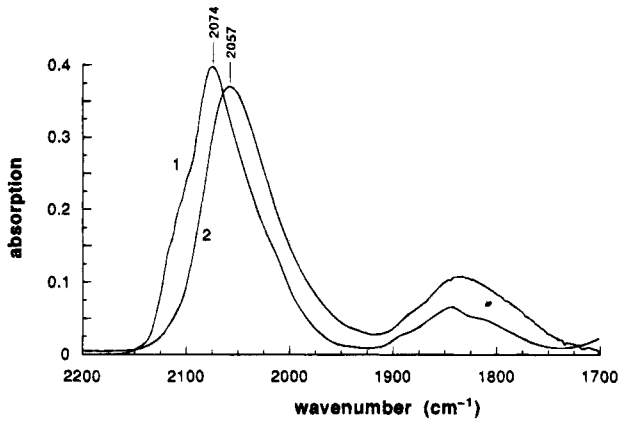

Figure 11. IR spectra of TPD-RT before (1) and after (2) overnight flush with water-contaminated helium.

3675 and 3780 cm^{-1} decrease in amplitude with increasing final TPD temperature.

To assess the effect of water adsorbed inside the zeolite on the IR absorption spectrum of both linear and multiple adsorbed CO, the spectra of TPD-RT and the spectrum of a Pt/H−LTL catalyst that was reduced at 300 °C, evacuated at RT, and saturated with water during overnight flushing with water contaminated helium are shown in Figure 11. The maximum of the linear absorption band shifts from 2074 to 2057 cm^{-1}, and the high-frequency shoulder of the linear CO band decreases upon adsorption of water. Simultaneously, the intensity of the peak associated with multiple adsorbed CO increases.

The presence of oxygen on the metal surface, as accomplished by slowly admitting oxygen to the reduced catalyst at 50 °C, affects the position and intensity of the absorption bands dramatically. After passivation the absorption in both the linear-CO band as well as the bridge-CO band region is diminished compared to TPD-300 (Figure 12). Concomitantly the high-frequency shoulder of the linear-CO band has gained intensity. The second derivative of the linear-CO band of the passivated sample shows the attenuation of the components and the increase of the component at 2142 cm^{-1} as well as the appearance of a new component at 2157 cm^{-1}.

To check the reversibility of the hydrogen desorption, additional TPD-300 and TPD-690 samples were heated in hydrogen to 300 °C followed by evacuation at RT and CO adsorption at RT. The difference spectra of TPD-30 with the thus obtained spectra are shown in Figure 13. TPD to 300 °C does not result in significant changes in the IR spectrum in both an absolute and a relative sense, suggesting that the desorption process does not bring about irreversible changes in the sample

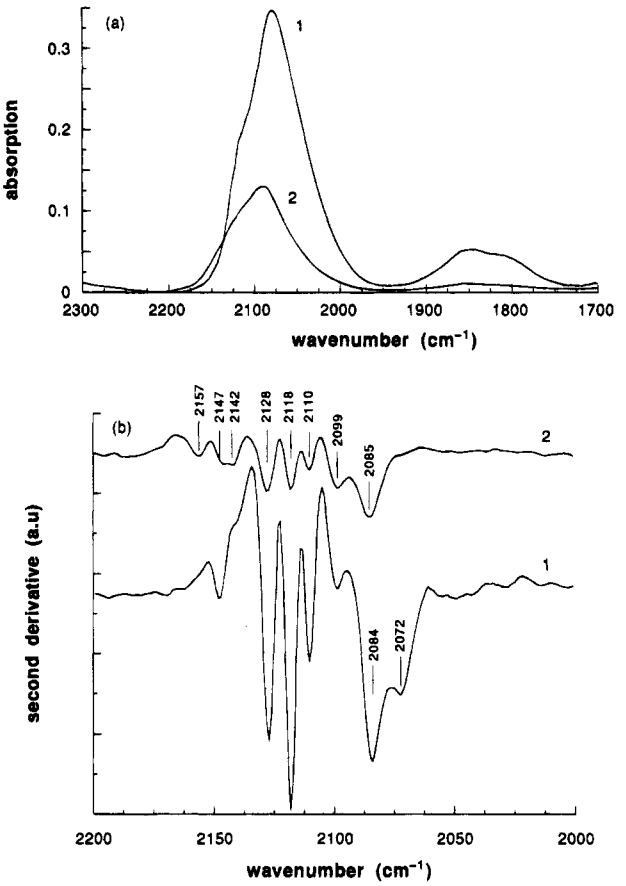

Figure 12. (a) Infrared spectra of CO adsorbed on TPD-RT (1) and Pt/H−LTL dried at 120 °C, reduced at 300 °C, and slowly exposed to oxygen at 50 °C (2). (b) Second derivatives of the spectra shown in (a).

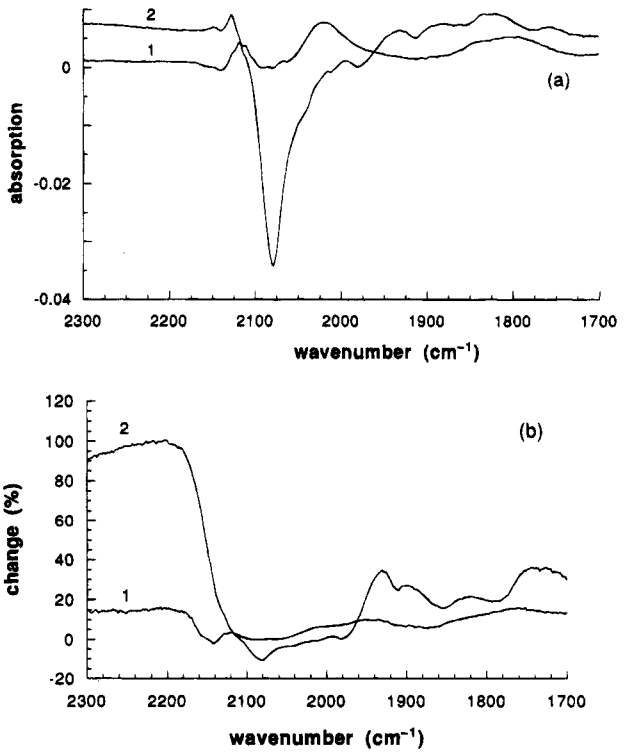

Figure 13. (a) Difference spectra of TPD-30 and TPD-300 (1) or TPD-690 (2) heated in H_2 to 300 °C and evacuated at RT after mimicking the TPD. (b) Same spectra as (a), but now in percentage difference.

up to 300 °C. The changes induced by TPD up to 690 °C are larger than the changes induced by TPD up to 300 °C, with the largest absolute difference in the linear-CO region. On a relative scale (Figure 13b) the differences in the linear-CO region are however small, suggesting that the metal particles are not significantly changed by the TPD. The decreased absorption above 2170 cm^{-1} is probably due to the desorption of water.

Discussion

Structure. The structure of the Pt/H−LTL catalyst after reduction at 300 °C, as well as after heating in helium to 500 or 690 °C, coincides with early[18,19,24,25] and recent[9] EXAFS studies of supported platinum catalysts. The average particle consists of 4 or 5 atoms after in-situ drying at 120 °C followed by reduction at 300 °C. Direct reduction,[9] i.e., no drying step, of this Pt/H−LTL catalyst at 300 °C results in slightly larger platinum particles ($N = 4.1$). Apparently, the presence of water in the zeolite pores affects the reduction chemistry of the $Pt(NH_3)_4^{2+}$ complex. The increase in particle size to ≈13 atoms during TPD is in agreement with the widely observed sintering of metal catalysts during treatment at high temperature.

The structure of the metal−support interface, i.e., a Pt−O distance in the range 2.5−2.7 Å in R-300 and a Pt−O distance below 2.3 Å for TPD-500 and TPD-690, agrees with more extensive studies.[9,17] The model that accounts for the shortening of the Pt−O distance proposes that after reduction at 300 °C hydrogen is present between the platinum particle and the support. This hydrogen desorbs at temperatures above 450 °C, bringing about a shortening of the Pt−O distance to ca. 2.2 Å when the platinum particles are covered with chemisorbed hydrogen.[2,9] In TPD-500 and TPD-690 the platinum particles are not covered with hydrogen, and a Pt−O distance of ca. 2.05 Å is determined. Metal−oxygen distances in this range have been reported for catalysts reduced at low or high temperature followed by treatment at temperatures above 450 °C in an inert atmosphere.[18,19,24] Apparently, chemisorbed hydrogen does affect not only the metal−metal distance in small metal particles but also the distance and interaction between the metal particle and the support. Although the coordination number is small, the Pt−O contributions have a significance of 92% and 72% in TPD-500 and TPD-690, respectively. The negative disorder values for the Pt−O contributions in TPD-500 and TPD-690 indicate a very uniform distance between the platinum and oxygen atoms. However, the low Pt−O coordination number suggests that this is only the case for a very small percentage of the platinum atoms. Additional evidence for this explanation comes from the high disorder values for the Pt−Pt contributions which suggests a high disorder in the platinum clusters.

The Pt−Pt distance (2.74 Å) in the platinum particles on which hydrogen is chemisorbed is slightly smaller than the bulk Pt−Pt distance (2.77 Å). A contraction of the metal−metal distance of approximately 0.10 Å has been measured[14−16] for small metal particles without chemisorbed hydrogen. Calculations showed that the contraction is due to the increased electrons density between the metal atoms.[26] Hydrogen chemisorption decreases the electron density between metal atoms[27] and therefore brings about a higher metal−metal bond length than for naked clusters. The extent to which the contraction due to the smallness of the cluster and the relaxation due to the chemisorption of hydrogen cancel each other results in the observed Pt−Pt distance of 2.74 Å for R-300. When no hydrogen in present on the surface of the platinum particle or in the metal−support interface (TPD-500 and TPD-690), the contraction of the Pt−Pt distance is 0.14 Å. This contraction is 40% larger than the contraction for Pt/γ-Al_2O_3 after reduction at 300 °C followed by evacuation at 300 °C (0.10 Å).[14,16] Evacuation at 300 °C removes all chemisorbed hydrogen but does not affect the interfacial hydrogen,[14,16] hydrogen between the metal particle and the support. Hence, after evacuation at 300 °C still some electron-withdrawing hydrogen is attached to the metal particle, bringing about the smaller contraction of the metal−metal distance after evacuation at 300 °C than after TPD up to 500 or 690 °C.

Electron Density Distribution. Three separate characteristics of X-ray absorption edges will be considered: (1) shape, (2) intensity, and (3) position of the edge. The shape is related to the distribution of the density of empty states.[28] The combined intensity of the L_{II} and L_{III} absorption edge is a measure for the number of holes in the valence band of the metal (2). The edge position is determined by the Fermi energy, the intensity, and the shape of the edge.[10]

Calculations[26] and ^{195}Pt NMR measurements[29] have revealed that the shape of the LDOS is significantly changed going from bulk metal to small metal particles. Additionally, ^{195}Pt NMR of bare and partly hydrogen covered platinum clusters[29] and calculations on the interaction of dihydrogen and hydrogen atoms with Ir_4 clusters[27,30] show that the LDOS of the d-band is broadened by the chemisorption of hydrogen on the metal clusters. This is in complete agreement with the observed shape of the Pt L_{II} and Pt L_{III} X-ray absorption edge of R-300 and R-500.

A combined intensity of the L_{II} and L_{III} absorption edge lower than the intensity of the edges in bulk metal indicates that the number of holes in the d-band of the sample is less than the number of holes in the bulk metal; i.e., the platinum atoms in R-300 have more holes in the d-band than bulk metal, and in TPD-500 and TPD-690 the platinum atoms have fewer holes in the d-band than bulk metal. Other experiments[14,16] revealed that the number of holes in the d-band of platinum atoms in a Pt/Al_2O_3 catalyst with chemisorbed hydrogen was higher than in bulk metal and lower than in bulk metal without chemisorbed hydrogen. Moreover, the effect was completely reversible. This brings about that although the platinum atoms in R-300, where the particles are covered with hydrogen, have more holes in the d-band than bulk metal, this is not necessarily true for "bare" platinum clusters supported by acidic zeolites. No chemisorbed hydrogen is present on the surface of the platinum particles or in the interface between the platinum particles and the zeolite for TPD-500 and TPD-690. Therefore, the edge intensities of TPD-500 and TPD-690 imply that the platinum atoms in these samples have fewer holes in the d-band than bulk metal. LDF[26] and HFS-LCAO[31] calculations on neutral clusters predicted fewer holes in the d-band of small metal particles than in the d-band of bulk metal. In contrast, calculations on charged clusters,[31] which were considered to be better comparable with clusters that had adsorbed an X-ray photon, predicted more holes in the d-band for charged small metal clusters. In contrast, XPS measurements of clean Pd clusters supported by acidic zeolite LTL[32] and Pt/Al_2O_3 catalysts[33] show that the binding energy (BE) of Pd 3d and Pt 4f electrons is higher than the BE in bulk metal or small metal particles on neutral or basic supports. Although the measured BE is not necessarily equal to the orbital energy due to relaxation processes, which are sensitive to particle size and environment, the increase in BE going from basic to acidic supports suggests that metal particles on acidic supports are electron-deficient. This disagreement is only apparent when one realizes what is actually measured by XPS and the intensity of an X-ray absorption edge. XPS probes the energy and density of occupied states, while the intensity of an X-ray absorption edge is determined by the number of empty states above the Fermi energy to which transition of the core level electron is

allowed. (This restriction is the origin of the lower intensity of the Pt L_{II} edge when compared with the Pt L_{III} edge.) Hence, the energy of an XPS photoelectron can be affected by a shift in the energy of the orbital from which the electron originates, a change in the relaxation processes, a shift in the Fermi energy, and a change in the work function, while the intensity of an L_{III} and L_{II} X-ray absorption edge is a function of the distribution of the d-band LDOS and the Fermi energy. The above suggests that the discrepancy between XPS and the intensity of the X-ray absorption edges is due to a different d-band LDOS, which is not measured by XPS and/or a change in relaxation processes for small metal particles, which is not probed by the intensity of the X-ray absorption edge.

Infrared Spectroscopy. Adsorption of carbon monoxide on Pt/H−LTL after desorption of chemisorbed hydrogen results in a shift to higher wavenumber of the absorption band maximum of linearly adsorbed CO. Also, the bridge-CO frequencies change, and a new bridge-CO band appears after treatment at high temperature. Small metal particles on supports expose a large number of different adsorption sites due to the different coordination number of the surface platinum atoms, the interaction between support and metal particle, and the possibility that CO adsorbed on the metal interacts with the support. Before the changes in the IR spectra can be related to changes in the properties of the platinum particles, it is necessary to determine the effect of the possible interaction of adsorbed CO with the support.

It has been suggested that carbon monoxide adsorbed onto oxidized and electron-deficient Pt and Pd adsorption sites gives rise to infrared bands in the region 2200−2100 cm^{-1}.[34] Surface oxidation (Figure 12) increased the absorption in the frequency region 2200−2135 cm^{-1} and poisoned the surface sites adsorbing CO with frequencies below 2135 cm^{-1}. The second derivative reveals the presence of a new band at 2157 cm^{-1} and a decrease in the magnitude of the bands below 2135 cm^{-1}. Since the spectra after hydrogen desorption up to 690 °C (Figure 8) do not resemble the spectrum after surface oxidation at 50 °C, it is inferred that the platinum particles are not oxidized by support protons during the TPD, consistent with the EXAFS results.

Saturation of the zeolite with water reduces the high-frequency shoulder (2150−2100 cm^{-1}) of the linearly adsorbed CO absorption band by more than 80% and shifts the absorption maximum to lower wavenumbers by 17 cm^{-1} (Figure 11). Literature data for CO adsorbed onto monovalent and bivalent cations[22] suggest that the bands at 2149 and 2141 cm^{-1} in Figure 9 may be due to Pt^{+}−CO complexes. Bands located at 2126, 2118, 2110, and 2101 cm^{-1} have been attributed to CO adsorbed on $Pt^{\delta+}$ species.[22] Since water adsorbs on the cations in the zeolite[35] and is unlikely to reduce Pt^{+}, the observed spectra do not fit in the assignment of the bands at 2149 and 2141 cm^{-1} to Pt^{+}−CO complexes. The change of the CO absorption spectrum upon water absorption strongly suggests that the high-frequency shoulder is due to either direct interaction of the CO with the cations in the zeolite or interaction of the cation with the platinum particle resulting in CO adsorption sites that have a limited ability to donate electrons in the CO $2\pi^*$ orbital, i.e., $Pt^{\delta+}$−CO species. Previously, the effect of water adsorption on the IR spectrum of Pt/K−LTL was reported.[35] Interaction of the terminal O of CO with cations in the zeolite channels shifts the frequency of the CO stretch vibration to lower wavenumbers by as much as 60 cm^{-1}.[35] Upon adsorption of water the CO stretch vibration shifted to higher wavenumbers. In contrast, Figure 11 shows that with the acidic zeolite used here a high-frequency band is observed in the absence of water and a shift to lower frequency upon adsorption of water. It is therefore inferred that the high-frequency shoulder is not due to the direct interaction of the terminal O of CO with cations. This of course raises the question by what mechanism the change in the IR spectrum of Pt/H−LTL upon adsorption of water is brought about. EXAFS,[36] XRD,[36] and quantum chemical studies[37] have shown that the charge compensating cations in zeolites move upon (de)hydration of the zeolite. More particular, in hydrated zeolite Y, the first coordination shell of charge compensating cation consisted entirely of oxygen atoms,[36] suggesting that in hydrated zeolites direct interaction between metal particles and cations is absent. The influence of neighboring cations on the interaction of small metal particles with CO has been studied extensively by quantum chemical calculations. Wimmer et al.[38] showed that the C−O stretch frequency shifts downward when a cation and the CO molecule are on the same side of a metal cluster. Jansen and van Santen[39] calculated an upward shift when the metal cluster is located between the CO molecule and the cation. The agreement between these latter calculations and the observed spectra suggests that the high-frequency shoulder is due to polarization of the metal particles by the cations of the support.

The shift to higher wavenumbers of the linear absorption band of CO with increasing final TPD temperature is consistent with the observed increase in particle size with EXAFS. Atoms in the surface of smaller particles have a lower coordination number than atoms in the surface of larger particles. A lower coordination number results in an increased electron density and hence a shift to lower frequency of the linear-CO band.[40] Hence, the observed shift to higher frequency of the maximum of the linearly adsorbed CO band can be explained by an increase in the particle size. The frequency of the peak associated with linearly adsorbed CO, i.e., 2071−2081 cm^{-1}, is close to the frequency observed for CO on a Pt(111) single-crystal surface, i.e., 2084 cm^{-1},[41] in agreement with the observed metallic state of the platinum by EXAFS.

Implications for High-Temperature Hydrogen Desorptions. The aim of the work presented here was to determine the effect of temperature-programmed desorption (TPD) up to 690 °C on the properties of platinum particles in acidic zeolite LTL in order to determine whether hydrogen desorptions above 500 °C are due to the oxidation of metal particles by zeolite hydroxyl groups. This was accomplished by determining the local structure around the platinum atoms from EXAFS before and after the TPD, calculating the number of holes in the d-band of the platinum atoms from the intensity of the Pt L_{II} and L_{III} X-ray absorption edges, and examining the interaction between the platinum atoms and CO with infrared spectroscopy. After reduction, i.e., before TPD, the platinum is metallic as indicated by the EXAFS, the white line intensity, and the infrared spectra. TPD to 690 °C does not affect the metallic state of the platinum but brings about changes in the particle size, the structure of the interface between the zeolite framework and the metallic platinum particle, the number and distribution of holes in the d-band, and the interaction of the platinum particles with CO. The metallic state of the platinum particles after TPD to 690 °C as indicated by EXAFS, the white line intensity, and the interaction with CO implies that hydrogen desorbing from metal on acidic zeolite does not originate from the oxidation of the metal by zeolite hydroxyl groups. Moreover, Figure 10 shows that the intensity of the IR absorption peaks associated with the hydroxyl groups in the zeolite decreases with final TPD temperature, in agreement with the measurements from which the oxidation of the metal by hydroxyl groups was suggested.[42] A decrease in the number of zeolite hydroxyl groups was also

reported for metal-free acidic zeolites upon heating at temperatures around 500 °C,[43] suggesting that the decrease in the intensity of the hydroxyl peak is due to a reconstruction of the (internal) zeolite surface.

Implications for Catalysis. The activity of metal particles for the breaking of carbon−carbon bonds in alkanes depends on the supporting material and the pretreatment of the catalyst. Specific activity (TOF) increases with support acidity[2,6,32,44] but decreases with increasing reduction temperature.[2] Modification of the catalytic activity of the small metal particles by the support is generally invoked to explain the relation between support acidity and catalytic activity. This model is strongly supported by the recently reported linear relationship between the $3d_{3/2}$ binding energy of Pd supported by basic, neutral, and acidic zeolite LTL and the apparent activation energy for the hydrogenolysis of propane or neopentane.[32] Desorption of strongly adsorbed hydrogen,[3] subsurface hydrogen,[4] and hydrogen located between the metal particle and the support[2,9] has been invoked to explain the decrease in hydrogenolysis activity with increasing reduction temperature. The Pt−O distance of 2.7 Å for R-300 and the Pt−O distance of ≈2.05 Å for TPD-500 and TPD-690 are in agreement with the model that hydrogen evolves from the metal−support interface at temperatures above 450 °C. Both IR and XANES show that the more intimate contact between metal particle and support results in a change in the electronic properties of the metal particle, which in turn is likely to affect the catalytic activity.

Conclusion

Both X-ray absorption and infrared spectroscopy of a Pt/H−LTL catalyst show that the platinum particles are metallic after reduction at 300 °C. After hydrogen desorption by heating in helium to 500 or 690 °C the platinum particles are still metallic but have grown from 4−5 atoms to ≈13 atoms. Simultaneously, the number of holes in the d-band of the platinum particles decreases to values lower than values of bulk platinum, and the linear CO band shifts to higher wavenumbers. These changes in electronic properties have been related to the change in the structure of the metal−support interface, which is reflected in the decrease of the Pt−O distance from 2.64 Å after reduction to 2.05 Å after hydrogen desorption.

References and Notes

(1) Menon, P. G.; Froment, G. F. *J. Catal.* **1979**, *59*, 138.

(2) Miller, J. T.; Meyers, B. L.; Modica, F. S.; Lane, G. S.; Vaarkamp, M.; Koningsberger, D. C. *J. Catal.* **1993**, *143*, 395.

(3) Menon, P. G.; Froment, G. F. *Appl. Catal.* **1981**, *1*, 31.

(4) Levy, P.-J.; Primet, M. *Appl. Catal.* **1991**, *70*, 263.

(5) Kramer, R.; Andre, M. *J. Catal.* **1979**, *58*, 287.

(6) Homeyer, S. T.; Karpinski, Z.; Sachtler, W. M. H. *J. Catal.* **1990**, *123*, 60.

(7) Dalmon, J. A.; Mirodatos, C.; Turlier, P.; Martin, G. A. In *Spillover of Adsorbed Species*; Pajonk, G. M., Teichner, S. J., Germain, J. E., Eds.; Elsevier: Amsterdam, 1983; p 169.

(8) Kampers, F. W. H.; Maas, T. M. J.; van Grondelle, J.; Brinkgreve, P.; Koningsberger, D. C. *Rev. Sci. Instrum.* **1989**, *60*, 2635.

(9) Vaarkamp, M.; Modica, F. S.; Miller, J. T.; Koningsberger, D. C. *J. Catal.* **1993**, *144*, 611.

(10) Mansour, A. N.; Cook, Jr., J. W.; Sayers, D. E. *J. Phys. Chem.* **1984**, *88*, 2330.

(11) McMaster, W. H.; Del Grande, N. K.; Mallet, J. H.; Hubbell, J. H. National Bureau of Standards Report UCRL-50174, Section 11, Rev 1, 1969.

(12) Brown, M.; Peierls, R. E.; Stern, E. A. *Phys. Rev. B* **1977**, *15*, 738.

(13) Vaarkamp, M.; Linders, J. C.; Koningsberger, D. C. *Physica B* **1995**, *208&209; Proc. XAFS VIII, Berlin*, 159.

(14) Vaarkamp, M. Ph.D. Thesis, Eindhoven University of Technology, Eindhoven, The Netherlands, 1993.

(15) Moraweck, B.; Clugnet, G.; Renouprez, A. J. *Surf. Sci.* **1979**, *81*, L631.

(16) Vaarkamp, M.; Koningsberger, D. C. Submitted for publication.

(17) Koningsberger, D. C.; Gates, B. C. *Catal. Lett.* **1992**, *14*, 271.

(18) Lagarde, P.; Murata, T.; Vlaic, G.; Freund, E.; Dexpert, H.; Bournonville, J. P. *J. Catal.* **1983**, *84*, 333.

(19) Lytle, F. W.; Greegor, R. B.; Marques, E. C.; Sandstrom, D. R.; Via, G. H.; Sinfelt, J. H. *J. Catal.* **1985**, *95*, 546.

(20) Samant, M. G.; Boudart, M. *J. Phys. Chem.* **1991**, *95*, 4070.

(21) Otten, M. M.; Clayton, M. J.; Lamb, H. H. *J. Catal.* **1994**, *149*, 211.

(22) Sheppard, N.; Nguyen, T. T. In *Advances in Infrared and Raman Spectroscopy*; Clark, R. G. H., Hester, R. E., Eds.; Heyden: London, 1978; p 67.

(23) De La Cruz, C.; Sheppard, N. *Spectrochim. Acta, Part A* **1994**, *50*, 271.

(24) Emrich, R. J.; Mansour, A. N.; Sayers, D. E.; McMillan, S. T.; Katzer, J. R. *J. Phys. Chem.* **1985**, *89*, 4261.

(25) Koningsberger, D. C.; Sayers, D. E. *Solid State Ionics* **1985**, *16*, 23.

(26) Delley, B.; Ellis, D. E.; Freeman, A. J.; Baerends, E. J.; Post, D. *Phys. Rev. B* **1983**, *27*, 2132.

(27) Sanchez Marcos, E.; Jansen, A. P. J.; van Santen, R. A. *Chem. Phys. Lett.* **1990**, *167*, 399.

(28) Mott, N. F. *Proc. Phys. Soc. London A* **1949**, *62*, 416.

(29) Tong, Y. Y.; van der Klink, J. J. *J. Phys. Chem.* **1994**, *98*, 11011.

(30) Biemolt, W.; Jansen, A. P. J.; van Santen, R. A. *Chem. Phys. Lett.* **1991**, *180*, 95.

(31) Ravenek, W.; Jansen, A. P. J.; van Santen, R. A. *J. Phys. Chem.* **1989**, *93*, 6445.

(32) Mojet, B. L.; Kappers, M. J.; Muijsers, J. C.; Niemantsverdriet, J. W.; Miller, J. T.; Modica, F. S.; Koningsberger, D. C. *Stud. Surf. Sci. Catal.* **1994**, *84*; *Proc. 10th Int. Zeolite Conf.*, 909.

(33) Kaushik, V. K. *Z. Phys. Chem. (Munich)* **1991**, *173*, 105.

(34) Juszczyk, W.; Karpinski, Z.; Ratajczykowa, I.; Stanasiuk, Z.; Zielinski, J.; Sheu, L.-L.; Sachtler, W. M. H. *J. Catal.* **1989**, *120*, 68.

(35) Kappers, M. J.; Vaarkamp, M.; Miller, J. T.; Modica, F. S.; Barr, M. K.; van der Maas, J. H.; Koningsberger, D. C. *Catal. Lett.* **1993**, *21*, 235.

(36) Dooryhee, E.; Catlow, C. R. A.; Couves, J. W.; Maddox, P. J.; Thomas, J. M.; Greaves, G. N.; Steel, A. T.; Townsend, R. P. *J. Phys. Chem.* **1991**, *95*, 4514.

(37) George, A. R.; Catlow, C. R. A.; Thomas, J. M. *Catal. Lett.* **1991**, *8*, 193.

(38) Wimmer, E.; Fu, C. L.; Freeman, A. J. *Phys. Rev. Lett.* **1985**, *55*, 2618.

(39) Jansen, A. P. J.; van Santen, R. A. *J. Phys. Chem.* **1990**, *94*, 6764.

(40) Kappers, M. J.; van der Maas, J. H. *Catal. Lett.* **1991**, *10*, 365.

(41) Olsen, C. W.; Masel, R. I. *Surf. Sci.* **1988**, *201*, 444.

(42) Tzou, M. S.; Teo, B. K.; Sachtler, W. M. H. *J. Catal.* **1988**, *113*, 220.

(43) Ward, J. W. In *Zeolite Chemistry and Catalysis*; Rabo, J. A., Ed.; American Chemical Society: Washington, DC, 1976; p 118.

(44) Boudart, M.; Dalla Betta, R. A. In *Proceedings of 5th International Congress on Catalysis, Palm Beach, 1972*; Hightower, J. H., Ed.; North-Holland: Amsterdam, 1973; p 1329.

JP951517D